Available online at www.sciencedirect.com
ScienceDirect
Journal of Fluorine Chemistry 128 (2007) 1012–1018
JOURNAL OF FLUORINE CHEMISTRY
www.elsevier.com/locate/fluor

Controlled fluorination of clays

A. Majid [a,*], S. Argue [a], D. Kingston [a], S. Lang [b]

[a] Institute for Chemical Process and Environmental Technology, National Research Council of Canada, Ottawa, Ontario K1A 0R9, Canada
[b] Steacie Institute for Molecular Sciences, National Research Council of Canada, Ottawa, Ontario K1A 0R9, Canada

Received 19 January 2007; received in revised form 25 April 2007; accepted 30 April 2007
Available online 3 May 2007

Abstract

The fluorination of clays by a mild fluorinating reagent, HPF_6 was investigated using a sample of bentonite. The reaction resulted in the fluorination at the aluminum sites to form octahedral aluminum oxyfluoride species. This led to considerable modification of the surface characteristics such as surface area, porosity and particle size of nano-clay particles. The fluorinated clay was characterized by X-ray powder diffraction, XPS, SEM, EDS, infrared spectroscopy and solid-state NMR.

Keywords: Aluminum oxyfluorides; Bentonite; Clays; Characterization; Fluorination; Hexafluorophosphoric acid

1. Introduction

Clay minerals, are an important, plentiful, and low-cost class of materials with unique swelling, intercalation, and ion-exchange properties. Their thermal stability, chemical inertness, and laminate structure make them suitable for numerous applications in such diverse fields as catalysis, adsorption and ion exchange. The diversity of the uses of clay minerals is increasing because of the progress in surface and chemical modification possibilities [1]. Swelling behavior, adsorption properties, colloidal and rheological phenomena can be optimized and adjusted to the intended uses. In addition to applications well-known for a long time, new uses are found and new type of materials are created.

The modification of clay minerals is often used to tune reactivity in the field of heterogeneous catalysis, and it is common for solid catalysts to be pretreated or chemically modified before the desired reactivity is observed. There are various methods for the modification of solid catalysts including: adsorption, ion exchange, reactions with acids, binding of inorganic and organic anions, mainly at the edges and dehydroxylation and calcination [2]. For example the addition of chlorine and/or fluorine to the surface of alumina has been shown to modify acidity and, subsequently, activity, for acid-catalyzed F/Cl halogen exchange [2–6], alkylation [7,8], isomerization [9,10] and cracking reactions [11].

Fluorination is considered to be an important treatment for catalysts to improve their catalytic activity. It is known to modify surface acidity and subsequently the reactivity [3–5,7–10,12]. For example, fluorinated alumina is generally more reactive as a catalyst in acid-catalyzed hydrocarbon reactions than alumina itself [13] and fluorinated silica has a higher cumene cracking rate than non-fluorinated silica [14].

The fluorination of clay minerals has also been extensively used to enhance their catalytic activity [6]. Several authors have reported on the changes in structure and catalytic properties of montmorillonite after activation by solutions of HF, NaF, KF, NH_4F, NH_4HF_2, $(NH_4)_3AlF_6$, $(NH_4)_2SiF_6$ and CF_3SO_3H [13,15–20]. In general, these investigators observed that activation results in an increase in the number of acid centers and, consequently, the application of the material to acid catalysis is facilitated. The drastic changes in activity that result from fluorine addition are believed to be associated with distinct structural changes [2]. The changes caused by fluorination are also accompanied by an increase in surface area and porosity.

The adsorbed or ion exchanged fluorine is easily lost at higher temperatures or by treatment with acids or alkalies [20]. Therefore, the modification by adsorption or ion exchange using alkali metal fluorides or fluorinated surfactants cannot be as effective as the insertion of fluorine into the structure of aluminosilicates by chemical reaction with fluorinating agents. Also, the fluorination mechanism depends strongly on the

* Corresponding author. Tel.: +1 613 993 2017; fax: +1 613 991 2384.
E-mail address: abdul.majid@nrc.gc.ca (A. Majid).

0022-1139/$ – see front matter.
doi:10.1016/j.jfluchem.2007.04.031

fluorinating agent [21]. Changing the fluorinating agents may also affect the surface sites that are attacked first during the initial fluorination reactions.

We have discovered that hexafluorophosphoric acid is a mild fluorinating reagent that allows the controlled fluorination of clays. Whereas, elemental fluorine and many electrophilic fluorinating agents are highly aggressive, unstable and require special equipment and care for safe handling, hexafluorophosphoric acid is much milder and can be operated safely and efficiently. In this communication we report the reaction of hexafluorophosphoric acid, HPF_6 with bentonite, a 2:1 layer clay mineral. We believe the use of HPF_6 for modifying the surface and structure of clay minerals to be a new process. The reaction of this fluorinating reagent with the clay minerals results in the fluorination at the aluminum sites to form octahedral aluminum oxyfluoride species. The modified bentonite has been characterized by X-ray powder diffraction, XPS, SEM, EDS, infrared spectroscopy, solid-state NMR, density, and surface area measurements.

2. Experimental

2.1. Materials and methods

A grey colored powder form of Na-bentonite (source: Wyoming, USA) and all other reagents used were obtained from Aldrich and used as received. The chemical composition of bentonite: SiO_2, 48.9%; Al_2O_3, 14.9%; Fe_2O_3, 3.0%; MgO, 2.2%; Na_2O, 1.8%; K_2O, 0.1%; CaO, 0.4% and approximate formula of $Na_{0.3}Al_{1.44}Fe_{0.19}Mg_{0.27}[Si_4]O_{10}(OH)_2$.

2.1.1. Procedure

Bentonite (10 g) was dispersed in 1 L of deionized water using an ultrasonic bath. The suspension was stirred with 100 mL of 5 M H_2SO_4 in order to increase its surface activity and to remove impurities [22]. The suspension was then centrifuged and the cake re-dispersed in fresh deionized water. The process of centrifugation and re-dispersion of the cake was repeated three times in order to remove impurities. The washed cake was transferred to a Teflon bottle and dispersed in a mixture of isopropyl alcohol and water (1:1). The contents were agitated overnight on a roller mill in the presence of 1/4 in. alumina balls. The suspension was screened to remove alumina balls and transferred to a 1 L Teflon beaker. Hexafluorophosphoric acid (10 mL of 60 wt.% solution in water, 67.9 mmol; molar ratio of acid washed bentonite:HPF_6 = ~22:67.9) was added to this slurry. The mixture was stirred using a Teflon coated magnetic stirring bar at room temperature for 24 h. The suspension was then centrifuged and the cake washed several times with isopropyl alcohol and dried at 200 °C in a vacuum oven. Isopropyl alcohol decreases the interaction of water with the pore wall during drying. This prevents agglomeration of clay particles resulting in higher surface area product [23].

2.2. Measurements

X-ray powder diffraction data were collected between 2θ = 5–70° with a scan rate of 2°/min at 21 °C and 33% RH, on a Scintag XDS 2000 with a theta–theta geometry and a copper X-ray tube. The diffractometer had a pyrolytic graphite monochromator in front of the detector. The samples were mounted on a zero background sample holder made of an oriented silicon wafer.

PAS-FTIR (photo-acoustic Fourier transform infrared spectroscopy) spectra were collected using a MTEC Model 300 photoacoustic detector combined to a Bruker IFS 66/S FTIR spectrometer. Five hundred scans were collected at a resolution of 8 cm^{-1} in the rapid scan mode. Sixty-four scans of carbon black were used as reference and helium was the purge gas.

^{29}Si NMR spectra were recorded at 40 MHz on a TecMag Apollo series spectrometer. Samples were spun at 4.5 kHz in zirconia rotors in a Doty 7 mm MASS probe. The 90° pulse length was 10 μs. A 10 s delay between pulses was found to be adequate, and spectra were accumulated overnight. ^{27}Al NMR spectra were recorded at 78 MHz on a Bruker AMX-300 spectrometer, using a Doty 5 mm mass probe, a 5 mm zirconia rotor and 8–8.5 kHz MASS. A pulse length of 1 μs was used, and 1000 scans were acquired, with a 0.5 s delay between scans. A noticeable probe background was subtracted. The chemical shifts of aluminum and silicon were referenced against external 1 M aqueous aluminum nitrate and neat tetramethyl silane (TMS), respectively. ^{19}F spectra were acquired at 376.6 MHz on a Bruker dsx400 spectrometer. Samples were packed in 5 mm silicon nitride rotors and spun at the magic angle at 10 kHz, in a probe supplied by Doty instruments. The 90° pulse length was 10 μs, but a shorter 3 μs pulse was used due to the 400 kHz sweep width. One thousand scans with a 5 s relaxation delay were acquired. No ^1H decoupling was applied. The chemical shift was referenced to external aqueous trifluoroacetic acid taken as −79 ppm relative to the more common standard of $CFCl_3$.

XPS was performed with a Physical Electronics (Perkin Elmer, Eden Prairie, MN, USA) model 550 instrument. Monochromatic Al Kα radiation was used. The dry samples were pressed into indium foil for analysis. Survey spectra were collected using pass energies of 188 eV, while high resolution spectra were recorded with a 22 eV pass energy. An electron flood gun was used to neutralize the charge during the experiment. Binding energies were referenced to the carbon–carbon bond, which was assigned a binding energy of 285 eV. Atomic compositions were estimated using a standard program provided with the instrument. During analysis, the pressure inside the instrument was always below 5×10^{-9} Torr (<0.7 μPa).

Scanning electron micrographs were recorded using a Hitachi Field Emission Scanning Electron Microscope (SEM) Model S-4800 fitted with an Oxford Inca Energy Dispersive Spectrometer (EDS) used for elemental analysis. The images were taken at 1.2 keV electron volts and a current of 10 μA. The working distance was 8 mm. Elemental analysis is semi-quantitative and is measured at a working distance of 15 mm with a 20 keV beam energy and 20 μA of current. An average of five determinations was carried out.

Specific surface areas, pore volumes and pore-size distributions were determined using a Micromeritics Gemini III 2375

Table 1
Physicochemical characteristics of untreated and treated bentonite

Sample ID	BET surface area ($m^2\ g^{-1}$)	Density ($g\ m^{-3}$)	Micropore area ($m^2\ g^{-1}$)	Pore diameter (nm)	Particle size (nm)	Elemental composition (w/w%)[a]									
						O	F	Na	K	Mg	Ca	Fe	Al	Si	Si:Al
Untreated bentonite	31 ± 1.1	2.7 ± 0.1	11.9	4.8	1400 ± 40	54	–	1.3	0.1	1.3	0.3	2.1	7.9	22.8	2.9
Acid treated bentonite	46 ± 1.0	2.4 ± 0.1	7.5	4.8	1386 ± 55	53	–	1.2	0.1	0.8	0.3	1.0	7.7	23.3	3.0
Fluorinated bentonite	67 ± 1.5	2.3 ± 0.1	0	6.2	485 ± 6	37.8	20.6	1.1	0.1	0.7	0.3	0.9	8.3	9.5	1.15

[a] From EDS analyses (average of five determinations).

apparatus, using nitrogen as adsorbent at 77 K. The application of the BET equation was used to obtain the adsorption data [24]. The pore-size distribution of the samples was calculated from desorption isotherms, and the BJH method was used for calculations [24–26]. The density of the materials was determined by a Pycnometry measurement with helium using Micromeritics Accupyc 1330 apparatus.

2.2.1. Particle size analysis

The particle size distribution of the samples was determined using highly diluted dispersions in 1% aqueous solution of Na_3PO_4. The measurements were performed using Malvern Zetasizer Model 3000HS particle analyzer, which is based on the principle of laser ensemble light scattering. The particles are introduced to the analyzer beam in a sample presentation cell located in the optical unit. For each sample, the mean value of five replicate determinations was calculated. Values reported are the mean value for two replicate samples.

3. Results and discussion

3.1. Physicochemical characterization

Table 1 compares the physicochemical characteristics of untreated and treated samples of bentonite. The elemental analyses show changes in the clay composition following treatments. Acid treatment alone resulted in a strong reduction of both MgO and Fe_2O_3 contents. The treatment with fluorinating agent led to a significant decrease in silica and a relative increase in alumina in addition to the incorporation of over 20% fluorine in the clay sample. There is almost 60% decrease in the Si:Al ratio after fluorination, resulting most probably from the decomposition of the smectite structure. One consequence of mineral transformations as a result of fluorination process, is the significant increase in specific surface area of fluorinated clay ($67\ m^2\ g^{-1}$) compared to untreated clay ($31\ m^2\ g^{-1}$) and acid washed clay ($46\ m^2\ g^{-1}$). Higher surface area of the fluorinated clay is consistent with its reduced particle size (485 ± 6 nm) as compared to the particle size of the parent bentonite (1400 ± 40 nm).

3.2. X-ray powder diffraction

Fig. 1 shows XRD patterns of acid treated and fluorinated bentonites as well as the parent bentonite. Based on a comparison of the reported XRD patterns for clay minerals it is apparent that untreated bentonite contains montmorillonite as the major clay mineral, with trace amounts of quartz and calcite [27–29]. The XRD results show that acid treatment caused significant structural changes of the bentonite particles which is consistent with previous observations [30]. Acid treatment affected mainly *d*(0 0 1) reflections because of the resulting disorder of arranged laminar sheets of montmorillonite [30]. The intensity of the (0 0 1) reflection peaks belonging to the main montmorillonite mineral decreased and broadened after acid treatment. A broad and weak peak at $2\theta = 19^\circ$ corresponding to amorphous silica and a sharp and strong peak at $2\theta = 28.2^\circ$ belonging to clinoptilolite [31] appeared in the acid treated sample. The quartz impurity present in the parent bentonite became more visible on acid treatment.

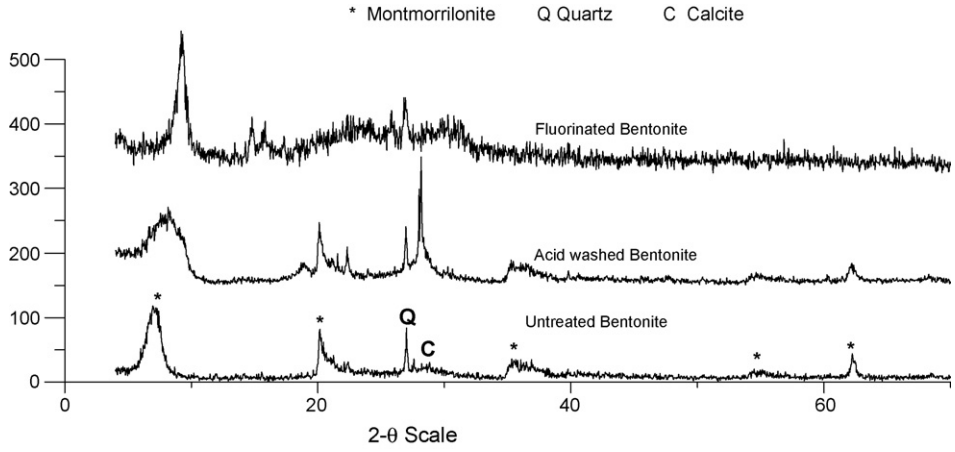

Fig. 1. XRD patterns for untreated and treated bentonites.

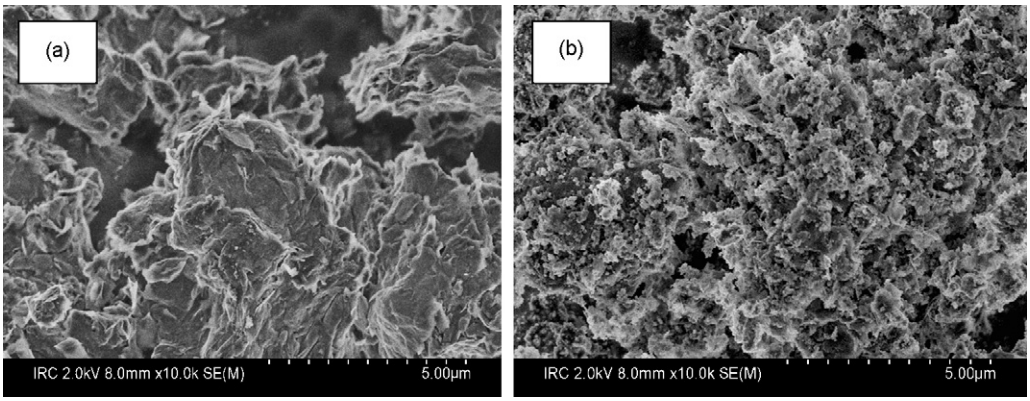

Fig. 2. SEM micrographs of: (a) untreated and (b) treated bentonites.

The XRD pattern of the fluorinated bentonite is significantly different from that of the acid treated and the parent bentonites. It essentially corroborate the absence of the characteristic montmorillonite reflections; suggesting that the structure was completely transformed. The characteristic peak for montmorillonite corresponding to the (0 0 1) plane and usually found [31] between $2\theta = 5^\circ$ and 10°, was found at a position of $2\theta = 7.1^\circ$ for parent bentonite and 7.8° for acid treated bentonite. It shifts to $2\theta = 9.3^\circ$ for fluorinated bentonite. The intensity of the (0 0 1) reflection peak was greatly increased and sharpened after fluorination. The diffraction pattern for fluorinated bentonite sample shows very broad peaks between $2\theta = 18^\circ$ and 32°, suggesting a loss of clay crystalline structure. The sharp reflections at $2\theta = 14.9^\circ$, 15.85°, and 25.6° could be due to aluminum fluoride hydroxyl hydrate phases [32,33]. The quartz impurity present in both parent and acid treated bentonite remained unaffected by fluorination.

3.3. Scanning electron microscopy (SEM)

Fig. 2 shows SEM micrographs of both untreated and treated bentonite samples. Both micrographs show crumpled platlets. More compacted aggregates are also observed. This is consistent with the reported SEM micrographs for bentonite [34,35]. However, smaller platlet sizes for the fluorinated samples compared to the untreated samples are clearly seen in the micrograph for treated sample.

3.4. Solid-state NMR spectroscopy

Nuclear magnetic resonance (NMR) spectroscopy has been shown to be capable of providing considerable information about the structures of aluminosilicates and clay minerals [36–41]. The position of silicon resonance is affected primarily by its degree of polymerization, and by the nature of the nearest neighbor cations, whereas the aluminum resonance is sensitive primarily to the number of atoms in its immediate coordination environment, i.e. to whether the aluminum is four- or six-fold coordinated by oxygen. Solid-state NMR is particularly sensitive to amorphous phases or small crystallites many of which cannot be detected by XRD.

Fig. 3 shows ^{29}Si MAS NMR spectra of the three bentonites. The spectrum of parent bentonite shows one major broad peak at −93 ppm and a sharper weak peak at −108 ppm. The major peak at −93 ppm can be assigned to the Si(0Al) environment, i.e. Si surrounded by three Si in the tetrahedral sheet [42,43]. The shoulder observed at −108 ppm is attributed to silicon atoms in the three dimensional silica network (Q^4 state) [41] and has been assigned to quartz impurity [44].

^{29}Si MAS NMR spectrum of the acid treated bentonite contains an additional small peak at −62 ppm in addition to an increase in the intensity of the Q^4 peak at −108 ppm. This peak can be attributed to a silicate impurity like olivine [45]. Compared with the parent bentonite, the acid washed bentonite

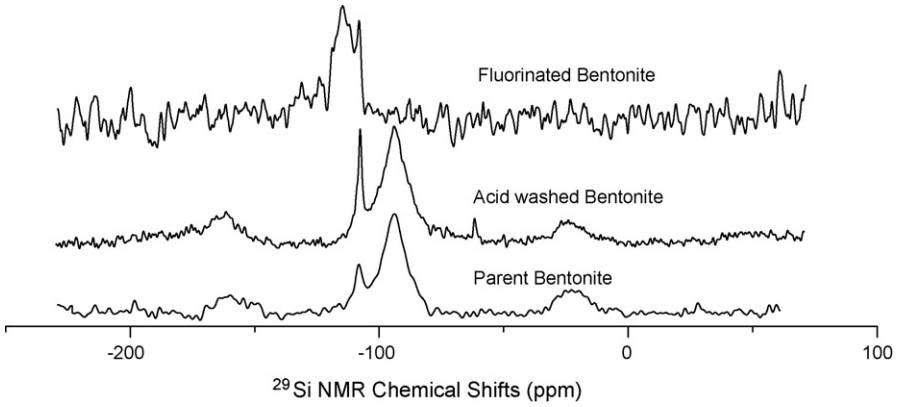

Fig. 3. ^{29}Si MAS NMR spectra of treated and untreated bentonites.

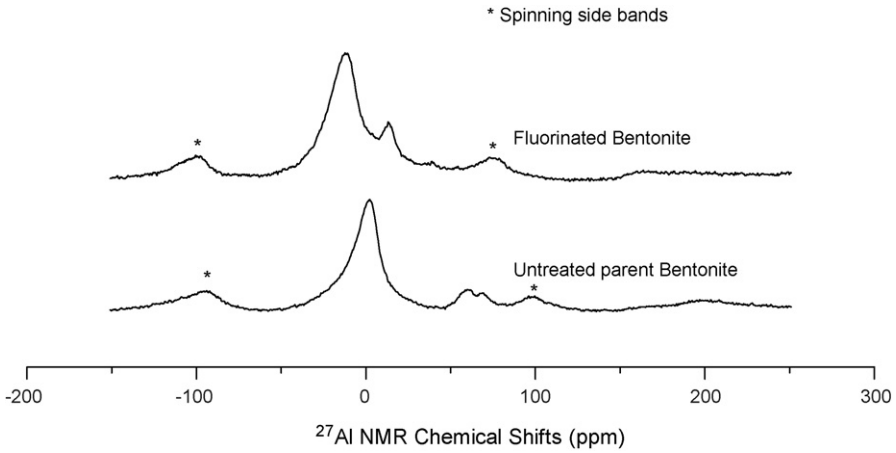

Fig. 4. ^{27}Al MAS NMR spectra of treated and untreated bentonites.

had a considerably reduced impurity of paramagnetic iron. This is expected to result in an improved spectral sensitivity and resolution thus explaining an increased Q^4 peak intensity at −108 ppm, and the emergence of a small new peak at −62 ppm in the ^{29}Si MAS NMR spectrum of acid washed bentonite [46]. Whereas there is no change in the position of Q^4 resonance either on acid treatment or fluorination, the Q^3 resonance shifts to Q^4 chemical shift range (−114 as against −93) on fluorination, suggesting the formation of amorphous silica [47]. The peak at −62 ppm observed in the acid treated bentonite disappears on fluorination.

The ^{27}Al MAS spectra of parent and fluorinated samples of bentonite, are shown in Fig. 4. A large peak at +2 ppm in the ^{27}Al NMR of parent bentonite indicates that much of the aluminum is in the octahedral Al environments [48–50]. This is in agreement with the ^{29}Si NMR spectra. Two poorly resolved peaks at 62 and 69 ppm are attributed to four-coordinate tetrahedral Al core [21,50]. As the fluorination process proceeds, all peaks shift to negative values, which are consistent with the formation of fluorinated species [21]. The major octahedral Al peak in the parent bentonite at 2 ppm is shifted to −9 ppm in the fluorinated bentonite, suggesting modification of the original smectite material, in which same coordination number for Al is maintained. This peak can be assigned to octahedral aluminum fluoride species [21,51]. The most apparent change is the shift of two poorly resolved resonances for four-coordinate tetrahedral Al species. The peak at 62 ppm in the ^{27}Al MAS NMR spectrum of parent bentonite moves to 14 ppm after fluorination. This suggests the formation of octahedral oxyfluoride species, $AlO_{6-x}F_x$ [48]. The peak at 69 ppm decreases in intensity and moves to 39 ppm. This region is usually assigned to five-coordinate Al [32,50].

^{19}F MAS NMR spectra shown in Fig. 5 indicate the presence of two major groups of resonances. The resonance represented by a broad strong peak centered around −130 ppm is consistent with octahedral aluminum oxyfluoride environments [48]. This could also be attributed to an Al–Al-vacancy environment, which is feature of the dioctahedral character of montmorillonites. A broad weak peak at −230 ppm could be assigned to terminal fluorine in tetrahedral or five-coordinate Al–F species [21,52–54].

3.5. Infrared spectra

In our previous investigations, we have demonstrated that compared with other IR techniques Step-scan Photoacoustic Fourier Transform Infrared (PAS-FTIR) is particularly suitable for the characterization of powder samples with strong IR absorption characteristics [55]. The technique is especially appealing because it requires neither vacuum nor special sample preparation techniques [56]. Fig. 6 shows PAS-FTIR spectra of both untreated and treated bentonites. The infrared spectra of parent and sulphuric acid washed bentonite were identical. After fluorination of bentonite, the structural OH stretching vibrations of clays at >3700 cm^{-1} do not present any significant changes, whereas the free –OH stretching of surface hydroxyl group at Al surface around 3630 cm^{-1} disappear and the νOH band around 3400 cm^{-1} usually assigned to adsorbed water [54] widens and increases in intensity. However, the 1650 cm^{-1} band, corresponding to the δOH vibration of water, remained unchanged, suggesting that the broad band around 3370 cm^{-1} may not represent contribution from adsorbed water, but could be due to formation of amorphous

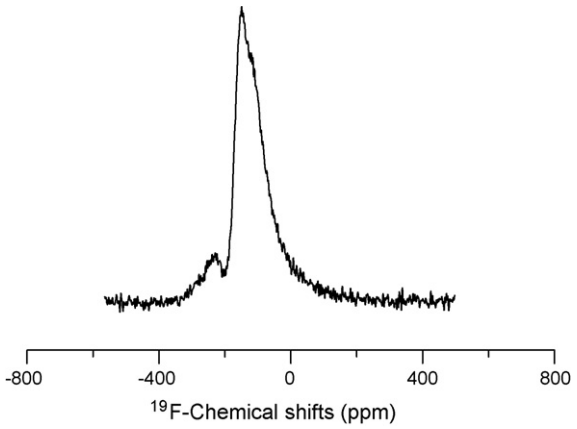

Fig. 5. ^{19}F MAS NMR spectra of fluorinated bentonite.

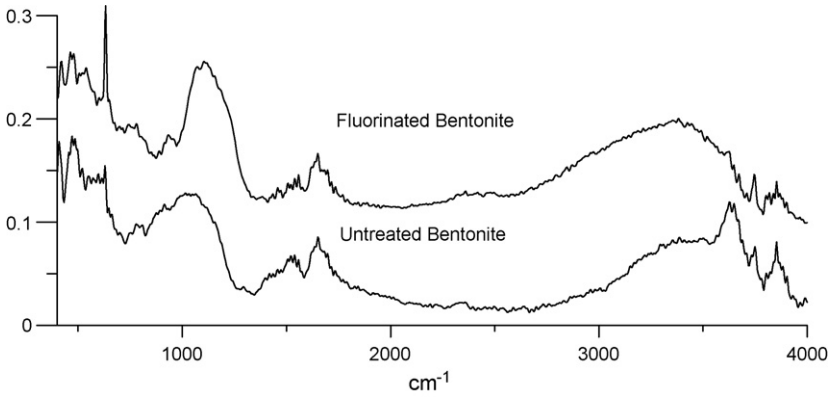

Fig. 6. PAS-FTIR spectra of untreated and treated bentonite.

aluminosilicate species [42]. The 915 cm^{-1} band (deformation δOH of Al–OH) [57] increases in intensity and shifts to 930 cm^{-1} which is characteristic for Al–Al–OH stretching in the octahedral layer [29]. The broad band around 1025 cm^{-1} corresponding to Si–O and Si–O–Si stretching bands becomes stronger and sharper on fluorination. The shifting of the band at 1025–1100 cm^{-1} coupled with the presence of a band at 3740 cm^{-1} (elongation vibration νOH of free Si–OH groups), and the emergence of a broad shoulder around 800 cm^{-1} suggests the formation of amorphous silica [57]. The intensity of the doublet at 460 cm^{-1} (Si–O–Al and Si–O–Mg coupled by OH vibrations or Si–O bending vibrations) decreased considerably with the emergence of a new band around 540 cm^{-1}, which has been assigned to Al–O–Si stretching mode [29]. A weak band at 630 cm^{-1} increases in intensity several folds. This is consistent with the formation of aluminum oxyfluoride species [58]. A weak doublet around 780 cm^{-1} which is characteristic of the presence of quartz [59], remains unchanged. This is consistent with the NMR data.

4. Conclusions

A methodology has been developed for the chemical fluorination of clays using a mild fluorinating agent, HPF_6. This approach resulted in the successful substitution of fluorine in a sample of bentonite leading to a substantial modification of not only the chemical composition, but its surface characteristics such as, surface area, porosity and particle size of nano-clay particles. Quartz present as an impurity in the parent clay did not react with the fluorinating agent.

The modification of the properties of bentonite on fluorination may have rendered the resulting fluorinated clay useful for several potential commercial applications such as: an additive for polymer nano-composites (PNCs, because of greater hydrophobicity) [60], heterogeneous catalysis (catalysts and catalysts support) [12,14,16], fuel cell (modification of proton exchange membranes, PEM) [61], for chemical and biological agent decontamination (by adsorption), for chemical, biological, radiological and explosives (CBRE), protective clothing (through filtration, adsorption or neutralization) after coating the clothing or additives with fluorinating clays.

References

[1] A.B. Bourlinos, D.D. Jiang, E.P. Giannelis, Chem. Mater. 16 (2004) 2404–2410.
[2] F. Bergaya, G. Lagaly, Appl. Clay Sci. 19 (2001) 1–3.
[3] E. Kemnitz, D.H. Menz, Prog. Solid State Chem. 26 (1998) 97–153.
[4] L.E. Manzer, Science 249 (1990) 31–35.
[5] L.E. Manzer, V.N.M. Rao, Adv. Catal. 39 (1993) 329–350.
[6] J. Fijal, M. Zyla, M. Tokarz, Clay Miner. 20 (1985) 81–92.
[7] L.M. Rodrigues, J. Alcraz, M. Hernandez, Y.B. Taaret, M. Variant, Appl. Catal. A 189 (1998) 15–21.
[8] L.M. Rodrigues, J. Alcraz, M. Hernandez, M. Dufaux, Y.B. Taaret, M. Variant, Appl. Catal. A 189 (1999) 53–61.
[9] Z. Cheng, V. Ponec, J. Catal. 148 (1994) 607–616.
[10] R. Covini, V. Fattore, N. Giordano, J. Catal. 7 (1967) 126–134.
[11] G.B. McViker, C.J. Kim, J.J. Eggert, J. Catal. 80 (1983) 315–327.
[12] C.V.A. Duke, J.M. Miller, J.H. Clark, A.P. Kybe, Spectrochim. Acta 46A (1990) 1381–1389.
[13] A.K. Ghosh, R.A. Kydd, Catal. Rev. Sci. Eng. 27 (1985) 539–589.
[14] J.H. Clark, A.P. Kybett, A.S. Piers, C.J. Williamson, J.M. Miller, in: H.A. Mottola, J.R. Steinmetz (Eds.), Chemically Modified Surfaces, Elsevier Science Publishers, 1992, pp. 193–207.
[15] M.J. Belzunce, S. Mendioroz, J. Haber, Clays Clay Miner. 46 (1998) 603–614.
[16] P. Dufresne, R. Malmaison, C. Marcilly, US Patent no. 4,766,099 (1988).
[17] K. Urabe, H. Sakurai, Y. Izami, J. Chem. Soc., Chem. Commun. (1988) 1520.
[18] K. Bruckman, J. Fijal, J. Haber, Z. Clapyta, T. Wiltoski, W. Zabinski, Mineralogia Pol. 7 (1976) 5–12.
[19] M. Yao, Z.Y. Liu, K.X. Wang, X.M. Hao, H.P. Tian, E.Y.A.O. Min, Chin. J. Catal. 25 (2004) 238–242.
[20] R.J. Hu, B.G. Li, Catal. Lett. 98 (2004) 43–47.
[21] P.J. Chupas, C.P. Grey, J. Catal. 224 (2004) 69–79.
[22] J.C. Dai, J.T. Huang, Appl. Clay Sci. 15 (1999) 51–65.
[23] A. Majid, S. Argue, V. Boyko, G. Pleizier, P. L'Ecuyer, S. Lang, J. Tunney, Colloids Surf. 224 (2003) 33–44.
[24] K.S.W. Sing, D.H. Everett, R.A.W. Haul, L. Moscou, R.A. Pierotti, J. Rouquerol, T. Siemieniewska, Pure Appl. Chem. 57 (1985) 603–619.
[25] M.L. Occelli, J.P. Olivier, J.A. Perdigon-Melon, A. Auroux, Langmuir 18 (2002) 9816–9823.
[26] G. Leofanti, M. Padovan, G. Tozzola, B. Venturelli, Catal. Today 41 (1998) 207–219.
[27] S.J. Chipera, D.L. Bish, Clays Clay Miner. 49 (2001) 398–409.
[28] J. Choi, C. Kang, J. Wang, J. Environ. Sci. Health A 36 (2001) 689–710.
[29] F.H. Lin, Y.H. Lee, C.H. Jian, J. Wong, M. Shieh, C. Wang, Biomaterials 23 (2002) 1981–1987.
[30] N. Yildiz, Z. Aktas, A. Climli, Particul. Sci. Technol. 22 (2004) 21–33.
[31] D.E.W. Vaughan, Catal. Today 2 (1988) 187–198.

[32] E.C. Decanio, J.W. Bruno, V.P. Nero, J.C. Edwards, J. Catal. 140 (1993) 84–102.
[33] J.M. Saniger, N.A. Sanchez, J.O. Flores, J. Fluorine Chem. 88 (1998) 117–125.
[34] J.P. Nguetnkam, R. Kamga, E. Villiéras, G.E. Ekodeck, A. Razafitianamaharavo, J. Yvon, J. Colloid Interf. Sci. 289 (2005) 104–115.
[35] M. Reinholdt, J. Miehe-Brendle, L. Delmotte, M.H. Tuilier, R. Dred, R. Cortes, A.N. Flank, Eur. J. Inorg. Chem. (2001) 2831–2841.
[36] N.C.M. Alma, G.R. Hays, A.V. Samoson, E. Lippmaa, Anal. Chem. 56 (1984) 729–733.
[37] P.F. Barron, M.A. Wilson, A.S. Campbell, R.L. Frost, Nature 299 (1982) 616–618.
[38] B.H.W.S. de Jong, C.M. Schramm, V.E. Parziale, Geochim. Coscochim. Acta 47 (1983) 1223–1236.
[39] J. Klinowski, J.M. Thomas, C.A. Fyfe, J.S. Hartman, J. Phys. Chem. 85 (1981) 2590–2594.
[40] E. Lippmaa, M. Magi, A. Samoson, M. Tarmak, G. Engelhardt, J. Am. Chem. Soc. 103 (1981) 4992–4996.
[41] R.A. Kinsey, R.J. Kirkpatrick, J. Hower, K.A. Smith, E. Oldfield, Am. Miner. 70 (1985) 537–548.
[42] S.R. Drachman, G.E. Roch, M.E. Smith, Solid State Nucl. Magn. 9 (1997) 257–267.
[43] J. Sanz, J.M. Serratosa, J. Am. Chem. Soc. 106 (1984) 4790–4793.
[44] G.E. Roch, M.E. Smith, S.R. Drachman, Clays Clay Miner. 46 (1998) 694–704.
[45] M. Magi, E. Lippmaa, A. Samoson, G. Engelhardt, A.R. Grimmer, J. Phys. Chem. 88 (1984) 1518–1522.
[46] M.J. Wilson, Clay Mineralogy, Chapman and Hall, London, 1994.
[47] T. Shinoda, M. Onaka, Y. Izumi, Chem. Lett. (Jpn.) 12 (1995) 495–496.
[48] G. Engelhardt, D. Michel, High Resolution Solid State NMR of Silicates and Zeolites, Wiley, New York, 1987.
[49] A.D. Irwin, J.S. Holmgren, J. Jonas, J. Mater. Sci. 23 (1988) 2908–2912.
[50] D. Mueller, D. Hoebbel, W. Gessner, Chem. Phys. Lett. 84 (1981) 25–29.
[51] H.M. Kao, Y.C. Chen, J. Phys. Chem. B 107 (2003) 3367–3375.
[52] H. He, J. Guo, X. Xie, H. Lin, L. Li, Clay Miner. 37 (2002) 337–344.
[53] N. Herron, D.L. Thorn, R.L. Harlow, F. Davidson, J. Am. Chem. Soc. 115 (1993) 3028–3029.
[54] K.H. Lim, F. Jousse, S.M. Auerbach, C.P. Grey, J. Phys. Chem. B 105 (2001) 9918–9929.
[55] B. Farid, A. Majid, Y. Deslandes, Spectrochim. Acta A: Mol. Biomol. Spectrosc. 57 (2001) 2695–2704.
[56] J.F. McClelland, R.W. Jones, S. Luo, L.M. Seaverson, in: P.B. Coleman (Ed.), Practical Sampling Techniques for Infrared Analysis, CRC Press, Boca Raton, FL, 1993 (Chapter 5).
[57] J. Pinkasa, H.W. Roeskyb, Organoaluminum Fluorides: J. Fluorine Chem. 122 (2003) 125–150.
[58] Y. Liu, J. Tossell, J. Phys. Chem. B 107 (2003) 11280–11289.
[59] L. Poppl, E. Toth, M. Toth, I. Paszli, V. Izvekov, M. Gabor, J. Therm. Anal. Calorimetry 53 (1998) 585–596.
[60] T.H. Elmer, I.D. Chapman, M.E. Nordberg, J. Phys. Chem. 67 (1963) 2219–2222.
[61] N.H. Jalani, K. Dunn, R. Datta, Electrochim. Acta 51 (2005) 553–560.